American Mineralogist, Volume 61, pages 1175–1193, 1976

Upper stability of chlorite + quartz in the system $MgO–FeO–Al_2O_3–SiO_2–H_2O$ at 2 kbar water pressure

PETER D. FLEMING[1] AND J. J. FAWCETT

Department of Geology, University of Toronto
Toronto, Canada

Abstract

The upper stability of chlorite + quartz assemblages at oxygen fugacities defined by the Ni–NiO buffer has been investigated at 2.07 kbar water pressure. Starting materials were oxide mixes, and in most of the later runs, crystalline products of earlier experiments. A variety of compositions was selected to intersect a wide range of chlorite–quartz tie lines. In the system $MgO–Al_2O_3–SiO_2–H_2O$ the assemblages stable below 590 ± 10°C are, with increasing alumina content, talc + chlorite + quartz, chlorite + quartz, cordierite + chlorite + quartz; above this temperature the stable assemblage is cordierite + talc + chlorite. For compositions with Fe/(Fe+Mg)= 0.5 in the system $MgO–FeO–Al_2O_3–SiO_2–H_2O$, the assemblages stable below 595 ± 10°C are, with increasing alumina content, talc + magnetite + chlorite + quartz, magnetite + chlorite + quartz, chlorite + quartz, cordierite + chlorite + quartz; the assemblage orthorhombic amphibole + cordierite + talc + magnetite is stable above about 600°C; although not delineated experimentally, the assemblage cordierite + talc + magnetite + quartz should be stable in a field occupying the narrow temperature interval between the chlorite–quartz assemblages and the amphibole–cordierite assemblage. For compositions with Fe/(Fe+Mg) = 0.082 and Fe/(Fe+Mg) = 0.75, the upper stability of chlorite + quartz is again close to 590°C. For the experimental conditions employed, the upper thermal stability of chlorite + quartz in a wide variety of assemblages is independent of both their alumina content and their Fe/(Fe+Mg).

Introduction

The assemblage chlorite + quartz is widespread in metamorphic rocks of very low (*e.g.* Coombs, 1954) to relatively high grades (*e.g.* Carmichael, 1970). In many rocks the breakdown of chlorite + quartz occurs before its maximum upper thermal stability by virtue of reactions with other phases such as muscovite, andalusite, and garnet. Reactions such as these are considered by many petrologists (*e.g.* Winkler, 1965, p. 101) to take place at or near the boundary between the greenschist facies and amphibolite facies, or, at lower pressures, between the albite–epidote hornfels and hornblende hornfels facies. Experimental studies on such reactions thus provide useful estimates of *PT* conditions at the facies transition (*e.g.* Seifert, 1970; Bird and Fawcett, 1973; Seifert and Schreyer, 1970; Hsu and Burnham, 1969). As a result of these reactions at lower temperatures, the simpler reactions of chlorite + quartz are not realized in many common rock types such as pelites, and only become important in those whose compositions approximate the less aluminous parts of $MgO–FeO–Al_2O_3–SiO_2–H_2O$ (Fig. 1). Nevertheless, experimental studies on the upper stability of chlorite + quartz assemblages can still provide useful, limiting estimates of the *PT* conditions experienced by some rocks. For example, the appropriate results might be applied as an additional estimate of the maximum possible temperatures experienced by the chlorite + quartz-bearing pelitic assemblages that are apparently stable well into the sillimanite zone of the Whetstone Lake area described by Carmichael (1970). This and other examples illustrate the point emphasized by Turner (1968, p. 127) that reactions representing the maximum thermal stability of chlorite + quartz are not diagnostic of facies boundaries (*cf.* Akella and Winkler, 1966, P. 10). Rocks that approximate part of the system $MgO–FeO–Al_2O_3–SiO_2–H_2O$, although not abundant, have been well

[1] Present Address: Department of Geology, University of Cape Town, Rondebosch 7700, Republic of South Africa.

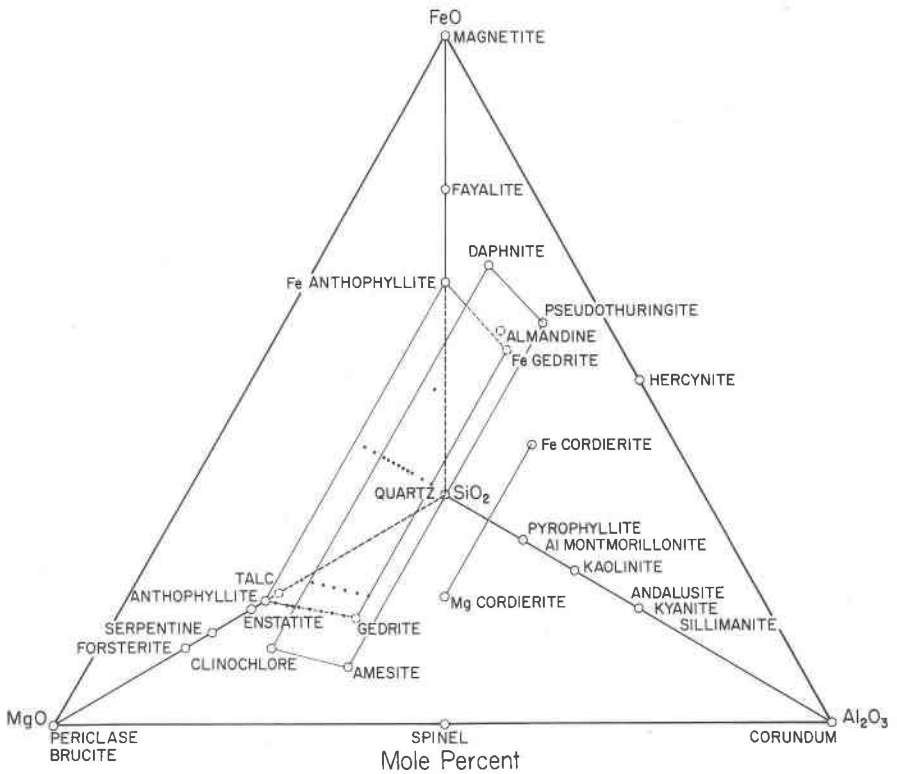

FIG. 1. Composition of a number of the phases in the system MgO–FeO–Al_2O_3–SiO_2–H_2O projected onto the H_2O-free tetrahedron. A line for cordierite and planes for orthorhombic amphibole and chlorite represent solid-solution ranges. Dots represent compositions of starting mixes.

documented from several localities (Eskola, 1914; Vallance, 1967; Froese, 1969; Lal and Moorhouse, 1969; Spence, 1969). These "cordierite–anthophyllite" rocks have often been shown to have unusually chlorite (± quartz)-rich antecedents, and results from experiments on chlorite + quartz can be usefully applied in the elucidation of their petrogenesis.

As part of an investigation of the system MgO–Al_2O_3–SiO_2–H_2O, Yoder (1952) studied the breakdown of clinochlore ($5MgO \cdot Al_2O_3 \cdot 3SiO_2 \cdot 4H_2O$) at 2 kbar water pressure, and with intervening contributions by others (notably Nelson and Roy, 1954, 1958; Roy and Roy, 1955), the work was later extended and elaborated by Fawcett and Yoder (1966). Hydrothermal work on the stability of iron chlorites began with the 2 kbar work of Turnock (1960) and has been continued at higher pressures by James *et al.* (1976), and the dehydration and breakdown of Mg–Fe chlorites of the clinochlore–daphnite ($5FeO \cdot Al_2O_3 \cdot 3SiO_2 \cdot 4H_2O$) series have been studied at 2 kbar water pressure by McOnie *et al.* (1975).

The studies of Fawcett and Yoder (1966) were the first to experimentally verify the existence of chlorite + quartz tie-line in their work on the upper stability of Mg chlorite + quartz at 2 kbar and 5 kbar P_{H_2O}. Their experiments were mainly of the synthesis type, with glasses as starting materials, and no good reaction reversals were obtained. Experiment products were chlorite + quartz below about 575°C and cordierite + talc at higher temperatures. Turnock's (1960) work in the system FeO–Al_2O_3–SiO_2–H_2O showed that the upper stability of Fe-chlorite + quartz is also at a temperature close to 575°C. It was noted by Fawcett and Yoder (1966) that the upper thermal stability of chlorite + quartz might be more or less independent of Fe/Mg ratio. The present work tests this proposition, and has determined the various stable assemblages and their phase relationships in the relevant part of the system MgO–FeO–Al_2O_3–H_2O. Part of Fawcett and Yoder's work in the system MgO–Al_2O_3–SiO_2–H_2O was repeated as well, except that the starting materials were oxide mixes and synthetic crystalline run products rather than glasses, in an attempt to obtain reaction reversals

TABLE 1. Composition of oxide mix starting materials in molecular proportions of oxides

Mix	MgO[1]	FeO[2]	Al_2O_3[3]	SiO_2[4]	Fe/Fe+Mg
2	6.5		0.5	7.5	0
3	6.25		0.75	7.25	0
4	6		1	7	0
5	5.75		1.25	6.75	0
6	5.5		1.5	6.5	0
7	5.25		1.75	6.25	0
8	5		2	6	0
10	5.85	0.52	0.5	7.5	0.082
11	5.625	0.5	0.75	7.25	0.082
12	5.4	0.48	1	7	0.082
13	5.175	0.46	1.25	6.75	0.082
14	4.95	0.44	1.5	6.5	0.082
15	4.725	0.42	1.75	6.25	0.082
16	4.5	0.4	2	6	0.082
18	3.25	3.25	0.5	7.5	0.5
19	3.125	3.125	0.75	7.25	0.5
20	3	3	1	7	0.5
21	2.875	2.875	1.25	6.75	0.5
22	2.75	2.75	1.5	6.5	0.5
23	2.625	2.625	1.75	6.25	0.5
24	2.5	2.5	2	6	0.5
26	1.5	4.5	1	7	0.75
27	6.75		0.25	7.75	0
28	6.375		0.625	7.375	0
29	3.375	3.375	0.25	7.75	0.5
30	3.0625	3.0625	0.875	7.125	0.5
31	2.9375	2.9375	1.125	6.875	0.5
32	2.8125	2.8125	1.375	6.625	0.5

[1] *From magnesium carbonate ($MgCO_3$), heated slowly in air, and held at about 1000°C for 5 hours.*

[2] *As Fe_2O_3; from ferrous oxalate ($Fe(COO)_2.2H_2O$), decomposed in final mix by heating for one hour at 300°C.*

[3] *δAl_2O_3; prepared from aluminum hydroxide ($Al(OH)_3.nH_2O$), using the method of Stirland et al. (1958).*

[4] *Acid washed, and 1150°C fired silica (SiO_2) powder.*

across the proposed phase boundaries. Preliminary data from these studies were presented by Fleming and Fawcett (1974).

Experimental methods

Starting materials

Starting materials were prepared for 28 mixtures that correspond to various anhydrous compositions in the orthoamphibole solid solution series anthophyllite–gedrite–ferroanthophyllite–ferrogedrite (except mixes 10–16, which had compositions very slightly more silica-rich than orthoamphibole compositions). The molecular proportions of oxides used in each mix are listed in Table 1, and the resulting compositions shown graphically on Figures 1 and 2. The range of compositions was selected to intersect chlorite–quartz tie lines over a wide range of bulk composition.

Oxides were each prepared in platinum crucibles from certified purity reagents, using the methods noted at the foot of Table 1. They were then weighed into mixtures, which, in the case of Fe-bearing compositions, were heated for one hour in air to decompose ferrous oxalate to Fe_2O_3. Thorough mixing of the oxides was then ensured by grinding under ace-

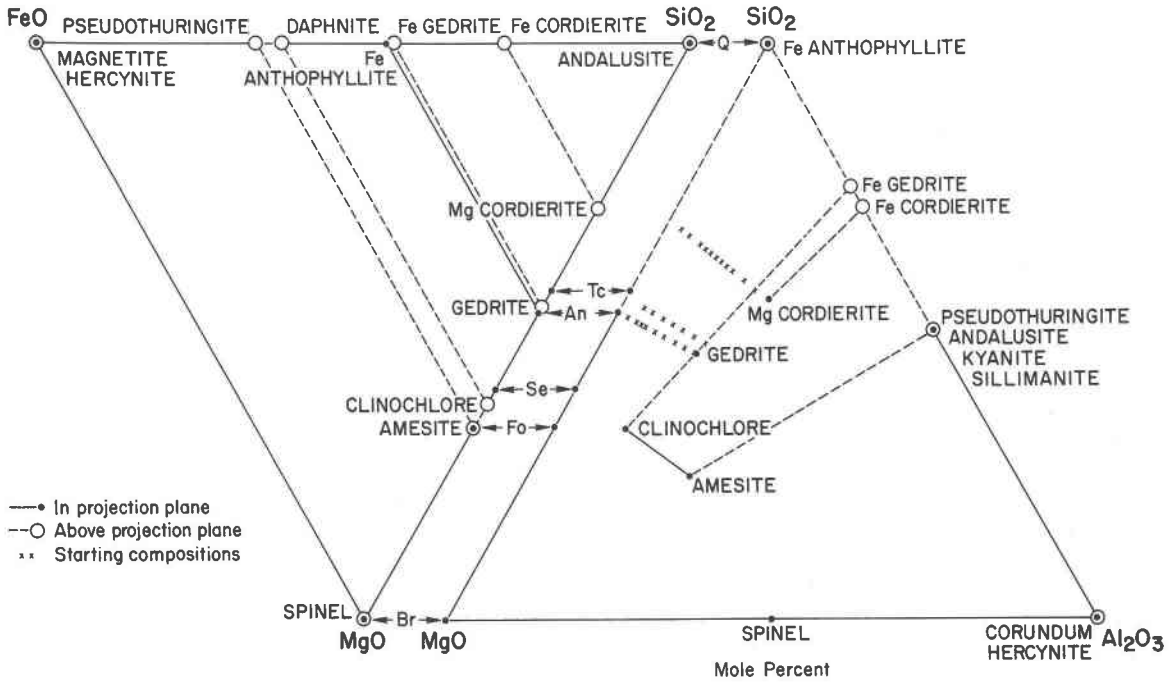

FIG. 2. Composition of a number of the phases in the system MgO–FeO–Al_2O_3–SiO_2–H_2O projected onto two faces of the tetrahedron of Fig. 1. The triangle at left is a projection from Al_2O_3 of some of the contents of the tetrahedron. The triangle at right is a projection from FeO of some of the contents of the tetrahedron, and is employed in Figs. 4 and 8. Crosses represent compositions of starting mixes.

tone for 4 hours in a mechanical mortar. Finally, the mixes were dried at 110°C for 24 hours.

As the work progressed, the reactants in many of the experiments were the products of earlier runs rather than the raw oxide mixes mentioned above.

Equipment and techniques

All runs were made at 30,000 p.s.i. (2.07 kbar), with water as the pressure medium. Equipment and techniques were essentially the same as those described in earlier papers from our laboratory (Bird and Fawcett, 1973; Grieve and Fawcett, 1974; McOnie *et al.*, 1975).

All results reported for the buffered experiments apply only to the charge contained inside the silver tube (Eugster and Wones, 1962). Temperatures could be controlled to within 5°C of the set point and were measured with chromel–alumel thermocouples (manufacturer's certified accuracy: ± 0.75 percent of measured temperature). The temperatures were automatically measured and recorded, usually at two-hourly intervals, by a multichannel data acquisition system, the Kaye System-8000.[2] Each temperature reported in this work is the mean temperature calculated from all temperatures recorded at regular 8-hour intervals (or 12 hours for some of the earlier runs) for the entire run duration. An uncertainty is also listed with each temperature, and was computed as the thermocouple accuracy correction plus two standard errors of the mean temperature (Eisenhart, 1968). Water leaks in pressure system were rare, but the run was aborted if its pressure dropped by more than 3 percent. The maximum combined error in precision and accuracy of the pressure measurement is less than ± 5 percent of the reported value.

Total run times varied from about 4 weeks for some of the Fe-free compositions up to about 27 weeks for some of the Fe-bearing compositions. Commonly, the longer experiments were quenched, examined, lightly ground by hand, and reloaded several times during the total run time. All experiments were quenched at constant 2 kbar pressure with a jet of compressed air that cooled the bomb to approximately 80°C in about two minutes.

Identification and description of phases

A combination of both optical and X-ray diffraction methods was used to identify products of the

[2] Kaye Instruments Inc., Cambridge, Massachusetts

experiments. In general, most products were very fine-grained (~ 0.001–0.005 mm). Nevertheless, after some experience, most or even all phases present could be optically identified in oil mounts. The majority of difficulties were encountered in distinguishing between very fine-grained (in the order of 0.001 mm) talc and chlorite, and also between fine-grained (0.01 mm) quartz and anhedral cordierite. On the other hand, in some runs, certain phases (*e.g.* amphibole and cordierite) identitified optically could not be discerned on the X-ray diffractograms, because of the small amount present and/or because their diffraction peaks were masked by strong peaks of other phases. Routine X-ray identification was performed with Fe radiation, using either a Philips diffractometer equipped with a focussing monochromator, or an Fe target Norelco diffractometer employing a Mn filter.

The following descriptions are intended only as an outline of the distinguishing features and general appearance of each phase.

Chlorite produced in these experiments generally shows the characteristic strong 14 Å and 7 Å basal reflections. In a few noncritical low-temperature runs only a 7 Å structure appeared to have crystallized. The chlorite generally formed very fine-grained masses in which individual grains were not readily discerned, and was often intimately intergrown with other fine-grained phases such as talc, quartz, and magnetite. Scanning electron microscope images of products from a few runs revealed that the chlorite is present as masses of fine, pseudohexagonal plates a few microns in diameter. In Fe-free charges the chlorite was colorless; in Fe-rich charges pale yellowish-green colors were characteristic. Some of the chlorites produced below about 500°C contained fine, colorless, high-relief inclusions of corundum(?). A number of such products were rerun, and the inclusions decreased in size and abundance and finally disappeared entirely.

Quartz was a common stable or metastable product and occurred as small anhedral grains usually intergrown with other phases.

Talc occurred in some charges as relatively coarse (0.05 mm), highly birefringent colorless flakes, but in many it formed very fine-grained (0.001 mm) admixtures with other phases. Its presence could generally be readily detected from its strong 9 Å (002) X-ray reflection.

Cordierite commonly could be recognized in the charge with the naked eye, forming large (up to 0.6 mm diameter), stubby, pseudohexagonal prisms. This morphology also led to optical identification of small amounts of fine cordierite in charges where diffractograms did not reveal its presence. In a few charges, small amounts of questionable anhedral cordierite could not always be unequivocally distinguished from quartz. Cordierite was colorless and generally inclusion-free in Fe-free charges; in Fe-bearing compositions a very faint pinkish tinge was evident under the microscope. Cordierites from a few of the Fe-bearing runs had a small core dusted with fine magnetite inclusions.

Orthorhombic amphibole was the only elongate prismatic to acicular phase recognized in the run products. It was always too small (often $\leq$ 0.005 mm long) for detailed optical examination, but larger prisms consistently exhibited parallel extinction, length-slow character, medium birefringence and relief, and a very pale yellowish color. Diffractograms from charges containing higher proportions of orthoamphiboles revealed relatively weak reflections in the 12 to 37° 2θ (FeKα) range that corresponded to orthorhombic amphibole reflections listed in the A.S.T.M. index of powder diffraction patterns (cards 16-401, 13-506).

Magnetite occurred generally as anhedral grains, fine granules, and dust. Approximate hercynite contents determined using the method of Turnock and Eugster (1962) did not exceed 10 mole percent. Those magnetites produced in long runs above 595°C were apparently pure Fe_3O_4.

Hematite was identified together with magnetite in a few noncritical runs below about 500°C. In rare cases, hematite had not been reduced to magnetite even after 100 days total run time. Apparently at temperatures below 500°C, the oxygen buffering action of Ni–NiO through the platinum wall of the outer sample capsule was not always completely effected over even such relatively long run times.

Results

A total of about 250 runs has been completed on the compositions listed in Table 1. The results for only the more critical runs have been listed in Tables 2 and 3, and plotted on Figures 3, 5, and 9.

Mixes with Fe-free compositions

The results for critical runs on Fe-free compositions are listed in Table 2, and are interpreted on a temperature–composition projection along the join anthophyllite ($7MgO \cdot 8SiO_2 \cdot 2H_2O$)–magnesian gedrite ($5MgO \cdot 2Al_2O_3 \cdot 6SiO_2 \cdot 2H_2O$) in Figure 3. The symbols in Figure 3 represent the assemblages inter-

preted as stable; additional phases persisted in some runs near boundary curves (Table 2). All assemblages contained water as one additional stable phase. Six reversal experiments (runs 157B, 158B, 159, 160, 161B, 163) produced only partial destruction of the higher-temperature assemblage Co + Tc + Chl,[3] but were nevertheless successful in closely bracketing at

[3] References to particular assemblages will hereafter employ the abbreviations noted at the foot of Tables 2 and 3.

TABLE 2. Critical run data for the upper stability limit of chlorite + quartz assemblages in Fe-free compositions at P_{H_2O} = 2.07 kbar.

Run No.	Temperature* (°C)	Duration (hours)	Reactants	Products**
	Mix 27 (6.75 MgO 0.25Al_2O_3 7.75 SiO_2)			
166	530.4 ± 4.3	1052	Mix	Tc+Chl
156	560.0 ± 4.4	1052	Mix	Tc+Chl
	Mix 2 (6.5 MgO 0.5Al_2O_3 7.5 SiO_2)			
72	460.0 ± 5.0	896	Mix	Tc+Chl+Q
74	499.8 ± 4.2	896	Mix	Tc+Chl+Q
168B	499.6 ± 3.9	2010	2 Product	Tc+Chl+(Q)
2	520.7 ± 4.6	933	Mix	Tc+Chl
137	520.8 ± 4.4	722	74 Product	Tc+Chl+Q(-)
9	570.6 ± 4.8	811	Mix	Tc+Chl
	Mix 28 (6.375MgO 0.625Al_2O_3 7.375 SiO_2)			
167	530.4 ± 4.3	1052	Mix	Tc+Chl+Q
155	560.0 ± 4.4	1052	Mix	Tc+Chl+Q
164	580.5 ± 4.7	1052	Mix	Tc+Chl+Q
	Mix 3 (6.25MgO 0.75Al_2O_3 7.25 SiO_2)			
67	584.9 ± 4.7	1896	Mix	Tc+Chl+Q
161B	585.0 ± 4.5	2010	125 Product	Co(-)+Tc(-)+Chl+Q(+)
125	604.2 ± 5.0	1156	67 Product	Co+Tc+Chl
69	649.8 ± 5.6	896	Mix	Co+Tc+Chl
128	675.2 ± 5.3	1157	69 Product	Co+Tc+Chl
	Mix 4 (6.0 MgO 1.0 Al_2O_3 7.0 SiO_2)			
73	460.0 ± 5.0	896	Mix	Chl+Q
75	499.8 ± 4.2	896	Mix	Tc+Chl+Q
4	520.3 ± 3.4	940	Mix	Tc+Chl+Q
11	570.6 ± 4.7	811	Mix	Tc+Chl+Q
18	585.4 ± 4.8	1954	Mix	Tc+Chl+Q
160	585.3 ± 4.6	1052	70 Product	Co(-)+Tc(-)+Chl(+)+Q
124	595.3 ± 4.7	1156	11 Product	Co+Tc+Chl
70	649.8 ± 5.6	896	Mix	Co+Tc+Chl
	Mix 5 (5.75 MgO 1.25 Al_2O_3 6.75 SiO_2)			
12	570.8 ± 4.7	792	Mix	Chl+Q
162	580.5 ± 4.5	1052	19 Product	Tc(-)+Chl(+)+Q
19	585.4 ± 4.8	1954	Mix	Tc+Chl+Q
159	585.3 ± 4.6	1052	71 Product	Co(-)+Tc(-)+Chl(+)+Q
49	610.0 ± 4.7	1252	Mix	Co+Tc+Chl+Q
71	649.8 ± 5.6	896	Mix	Co+Tc+Chl

* *Uncertainty calculated as: 0.0075 of mean temperature + 2 standard errors of mean temperature. See text.*

** *Abbreviations: Co, cordierite; Chl, chlorite (14 Å); Chl_7, chlorite (7 Å); Q, quart; Tc, talc; (+) indicates that the amount of the phase increased with increasing run time; (-) indicates a decrease with increasing run time. Parentheses ( ) enclosing a phase indicate a trace amount was present. All assemblages contained water as an additional phase.*

*** *Mixes are listed in order of increasing alumina content (See Table 1 for compositions). Run data for each mix are listed in order of increasing temperature.*

TABLE 2. continued

Run No.	Temperature* (°C)	Duration (hours)	Reactants	Products**
		Mix 6 (5.5 MgO 1.5 Al_2O_3 6.5 SiO_2)		
13B	570.4 ± 4.7	2044	Mix	Chl+Q
163	580.5 ± 4.5	1052	50B Product	Co(-)+Tc(-)+Chl(+)+Q
20	585.4 ± 4.8	1954	Mix	Chl+Q
158B	585.0 ± 4.5	2010	126 Product	Co(-)+Tc(-)+Chl(+)+Q
51	595.1 ± 4.7	1252	Mix	Chl+Q
122	595.3 ± 4.7	1156	77 Product	Co+Tc+Chl
126	604.2 ± 5.0	1156	20 Product	Co+Tc+Chl
50B	609.8 ± 4.9	2764	Mix	Co+Tc+Chl
77	609.8 ± 4.9	1512	51 Product	Co+Tc+Chl
		Mix 7 (5.25 MgO 1.75 Al_2O_3 6.25 SiO_2)		
129B	560.0 ± 4.5	2209	14B Product	Co+Chl+Q
14B	570.4 ± 4.7	2044	Mix	Co+Chl+Q
52	595.1 ± 4.7	1252	Mix	Co+Chl+Q
127	604.2 ± 5.0	1156	52 Product	Co+Tc+Chl
		Mix 8 (5 MgO 2 Al_2O_3 6 SiO_2)		
8	519.5 ± 4.4	1816	Mix	Chl+Q
165	530.4 ± 4.3	1052	8 Product	Co+Chl+Q
68B	585.3 ± 4.5	2948	Mix	Chl+Q
157B	585.0 ± 4.5	2010	123 Product	Co(-)+Tc(-)+Chl(+)+Q
53	595.1 ± 4.7	1252	Mix	Co+Chl+Q
123	595.3 ± 4.7	1156	78 Product	Co+Tc+Chl
78	609.8 ± 4.9	1512	53 Product	Co+Tc+Chl

590°C the reaction chlorite + quartz = talc + cordierite + vapor, limiting the upper stability of assemblages containing chlorite + quartz. The results of two other reversal experiments on lower-temperature curves are also shown on Figure 3.

The results are essentially similar to those obtained by Fawcett and Yoder (1966) from experiments on glasses, but combining both sets of results, the configuration of curves shown in Figure 3 satisfies the results better than that of Fawcett and Yoder (1966, Fig. 4, p. 372). Relative to Figure 4 of these authors, the present configuration places the upper stability of chlorite + quartz about 15°C higher, and at temperatures higher than about 500°C, restricts the field for the assemblage Tc + Chl to slightly less aluminous compositions.

Chernosky (1975) has recently determined the upper stability of the clinochlore + quartz assemblage at water pressures from 0.5 to 4 kbar. At 2 kbar the temperature of the curve was stated to be 527° ± 10°C. (A better determination is now thought to be 513° ± 10°C, Chernosky, personal communication.) Our data do not give a very precise estimate of this same point. The clinochlore + quartz join projects onto Figure 3 approximately midway between mix numbers 4 and 5. For that composition Figure 3 shows an upper temperature limit for the chlorite plus quartz field of about 565°C. The controls on this curve are not good, and it may be necessary to modify its slope to accommodate Chernosky's data. According to our data, however, Chernosky should not have encountered cordierite below temperatures of about 590°C at 2 kbar.

The phase relations are conveniently illustrated by the series of isothermal sections of the system MgO–Al_2O_3–SiO_2–H_2O shown in Figure 4. Construction of compatibility triangles has been completed using appropriate data of earlier workers as noted in the figure caption. With respect to Figures 3 and 4, the comments and discussion of Fawcett and Yoder (1966, p. 368–377) are still generally appropriate, and most will not be repeated here. However, a few comments on the compositions of coexisting phases will be made below.

From Figures 3 and 4 it can be deduced that the alumina content of chlorite in equilibrium with quartz + talc increases slightly with temperature, whilst the chlorite in equilibrium with cordierite + quartz decreases markedly in alumina content. The compositional range of chlorites in equilibrium with quartz (only) narrows correspondingly, and at the upper stability of chlorite + quartz (590°C) a single composition, $clinochlore_{86}amesite_{14}$, obtains. It should be noted that although Figure 4 indicates that

TABLE 3. Critical run data for the upper stability limit of chlorite + quartz assemblages in Fe-bearing compositions at P_{H_2O} = 2.07 kbar, buffered with Ni–NiO

Run No.	Temperature* (°C)	Duration (hours)	Reactants	Products**
Compositions with Fe/Fe+Mg = 0.082				
Mix 10 (5.85 MgO 0.52 FeO 0.5 Al_2O_3 7.5 SiO_2)				
30	550.1 ± 4.3	1128	Mix	Tc+Chl+(Q)
38	600.6 ± 5.0	1296	Mix	Tc+Chl
Mix 11 (5.625 MgO 0.5 FeO 0.75 Al_2O_3 7.25 SiO_2)				
31	550.2 ± 4.5	1128	Mix	Tc+Chl+Q
Mix 12 (5.4 MgO 0.48 FeO 1.0 Al_2O_3 7.0 SiO_2)				
24	499.6 ± 4.1	840	Mix	Tc+Chl+Q
32	549.4 ± 4.4	1130	Mix	Tc+Chl+Q
Mix 13 (5.175 MgO 0.46 FeO 1.25 Al_2O_3 7.0 SiO_2)				
25	499.6 ± 4.2	834	Mix	Chl+Q
33	550.5 ± 4.1	1130	Mix	Chl+Q
195	579.7 ± 4.5	1343	Mix	Chl+Q
189	590.4 ± 4.7	1343	25 Product	Co+Tc+Chl+Q
41B	600.1 ± 4.6	2252	Mix	Co+Tc+Chl+Q(-)
Mix 14 (4.95 MgO 0.44 FeO 1.5 Al_2O_3 6.5 SiO_2)				
34	550.5 ± 4.4	1131	Mix	Chl+Q
42	600.0 ± 4.8	910	Mix	Co+Tc+Chl+Q
Mix 15 (4.725 MgO 0.42 FeO 1.75 Al_2O_3 6.25 SiO_2)				
35	550.0 ± 4.8	1131	Mix	Chl+Q
Mix 16 (4.5 MgO 0.4 FeO 2.0 Al_2O_3 6.0 SiO_2)				
28	500.2 ± 4.4	1106	Mix	Chl+Q
44	600.1 ± 5.2	910	Mix	Co+Tc+Chl+Q
Compositions with Fe/Fe+Mg = 0.5				
Mix 29 (3.375 MgO 3.375 FeO 0.25 Al_2O_3 7.75 SiO_2)				
140	550.1 ± 4.4	1440	Mix	Tc+Mt+Chl+Q
197	589.8 ± 4.7	1010	140 Product	Tc+Mt+Chl+Q
141C	600.6 ± 4.8	2343	Mix	Oa+Co+Tc+Mt+Chl+Q(-)
142B	650.0 ± 5.0	1775	Mix	Oa+Co(+)+Tc(+)+Mt(+)+(Q)(-)
Mix 18 (3.25 MgO 3.25 FeO 0.5 Al_2O_3 7.5 SiO_2)				
99	450.1 ± 3.7	1268	Mix	Tc+Mt+Hm+Chl+Q
61	501.2 ± 4.3	1494	Mix	Tc+Mt+Chl+Q
154	590.1 ± 4.6	1414	120B Product	Tc+Mt+Chl+Q
120B	649.7 ± 5.5	2189	61 Product	Oa+Co(+)+Tc(+)+Mt(+)+(Q)(-)
Mix 19 (3.125 MgO 3.125 FeO 0.75 Al_2O_3 7.25 SiO_2)				
79	450.4 ± 3.6	2904	Mix	Mt+Hm+Chl+Q
64	499.7 ± 4.1	1656	Mix	Tc+Mt+Chl+Q
101	525.5 ± 4.1	1268	Mix	Tc+Mt+Chl+Q
65	550.2 ± 4.4	1493	Mix	Tc+Mt+Chl+Q
100	599.3 ± 5.0	1268	65 Product	Oa+Co+Tc+Mt+Chl+Q
121C	650.2 ± 5.1	3288	101 Product	Oa+Co+Tc+Mt

* *Uncertainty calculated as for Table 2.*

** *Abbreviations: Oa, orthorhombic amphibole; Mt, magnetite; Hm, hematite; (?), presence of phase is uncertain; other abbreviations as for Table 2. All assemblages contained water as an additional phase.*

*** *Mixes and run data within each constant Fe/Fe+Mg set are grouped according to the scheme noted in Table 2.*

TABLE 3. continued.

Run No.	Temperature* (°C)	Duration (hours)	Reactants	Products**
	Mix 30 (3.0625 Mg0 3.0625 Fe0 0.875 Al_2O_3 7.125 SiO_2)			
143	500.4 ± 3.9	768	Mix	Mt+Chl+Q
144	550.8 ± 4.3	768	Mix	(Tc)+Mt+Chl+Q
145	574.9 ± 4.6	768	Mix	(Tc)+Mt+Chl+Q
171C	630.2 ± 4.8	2688	Mix	Oa+Co+Tc+Mt
	Mix 20 (3.0 Mg0 3.0 Fe0 1.0 Al_2O_3 7.0 SiO_2)			
81	550.1 ± 4.4	1270	Mix	Mt+Chl+Q
82	574.9 ± 4.6	1270	Mix	Mt+Chl+Q
153	589.9 ± 4.7	1414	82 Product	(Tc)+Mt+Chl+Q
80D	600.1 ± 4.7	4556	Mix	Oa+Co+(Tc)+Mt+Chl+Q(-)
83C	650.4 ± 5.2	3337	Mix	Oa+Co+Tc+Mt
	Mix 31 (2.9375 Mg0 2.9375 Fe0 1.125 Al_2O_3 7.125 SiO_2)			
194	583.0 ± 4.7	1342	172B Product	Oa(-)Co(-)+Tc (-)+Mt+Chl+Q
172B	630.4 ± 5.1	1364	Mix	Oa+Co+Tc+Mt
	Mix 21 (2.875 Mg0 2.875 Fe0 1.25 Al_2O_3 6.75 SiO_2)			
183B	585.5 ± 4.6	1576	84B Product	Oa(-)+Co(-)+Tc(-)+Mt (-)+Chl(+)+Q(+)
84B	600.4 ± 5.0	2354	Mix	Oa+(+)+Co(+)+Tc(+) +Mt(+)+Chl(-)+Q(-)
	Mix 32 (2.8125 Mg0 2.8125 Fe0 1.375 Al_2O_3 6.625 SiO_2)			
146	550.1 ± 4.4	768	Mix	(Mt)+Chl+Q
147	570.4 ± 4.5	767	Mix	(Mt)+Chl+Q
148	585.2 ± 4.6	1768	Mix	Chl+Q
	Mix 22 (2.75 Mg0 2.75 Fe0 1.5 Al_2O_3 6.5 SiO_2)			
91	450.6 ± 3.7	2400	Mix	Mt+Hm+Chl+Q
149	525.1 ± 4.1	1416	89 Product	Mt+Chl+Q
89	550.4 ± 4.6	1272	Mix	Chl+Q
196	580.0 ± 4.5	1009	91 Product	Chl+Q
88	600.0 ± 4.6	1272	Mix	Co+(Tc)+(Mt)+Chl+Q
132C	510.2 ± 4.8	2688	88 Product	Oa+Co+Tc+Mt
	Mix 23 (2.625 Mg0 2.625 Fe0 1.75 Al_2O_3 6.25 SiO_2)			
95	449.8 ± 3.6	1271	Mix	(Mt)+Hm+Chl+Q
150	465.0 ± 3.6	1440	94 Product	(Mt)+Chl+Q
135	474.9 ± 3.7	1440	95 Product	Chl+Q
94	499.9 ± 3.9	1693	Mix	Chl+Q
93	550.1 ± 4.3	1693	Mix	Chl+Q
182B	559.9 ± 4.3	1967	150 Product	Co+Chl+Q
152	589.9 ± 4.6	1414	93 Product	Co+Chl+Q
92	600.5 ± 4.8	1268	Mix	Oa(?)+Co+(Tc)+(Mt)+Chl
	Mix 24 (2.5 Mg0 2.5 Fe0 2.0 Al_2O_3 6.0 SiO_2)			
116	450.4 ± 3.8	1419	Mix	Chl_7+Q
98	500.0 ± 4.2	767	Mix	Chl+Q
181B	540.2 ± 4.2	1967	116 Product	Co+Chl+Q
151	589.7 ± 4.9	1414	Mix	Co+Chl+Q
96	599.5 ± 4.7	719	Mix	Oa(?)+Co+(Tc)+(Mt)+Chl
134C	609.7 ± 5.2	2686	96 Product	Oa+Co+Tc+Mt
176B	650.1 ± 5.1	2418	98 Product	Oa+Co+Tc+Mt
Compositions with Fe/Fe+Mg = 0.75				
	Mix 26 (1.5 Mg0 4.5 Fe0 1.0 Al_2O_3 7.0 SiO_2)			
185	570.1 ± 4.5	958	Mix	Mt+Chl+Q
192	580.2 ± 4.7	1340	Mix	Mt+Chl+Q
186	590.2 ± 4.8	958	Mix	Co(?)+Mt+Chl+Q
191	600.1 ± 4.7	1342	Mix	Co+Mt+Chl+Q
187	610.4 ± 5.0	958	Mix	Oa+Co+Mt+Chl+Q
188	630.5 ± 5.0	958	Mix	Oa+Co+Mt+Chl+Q

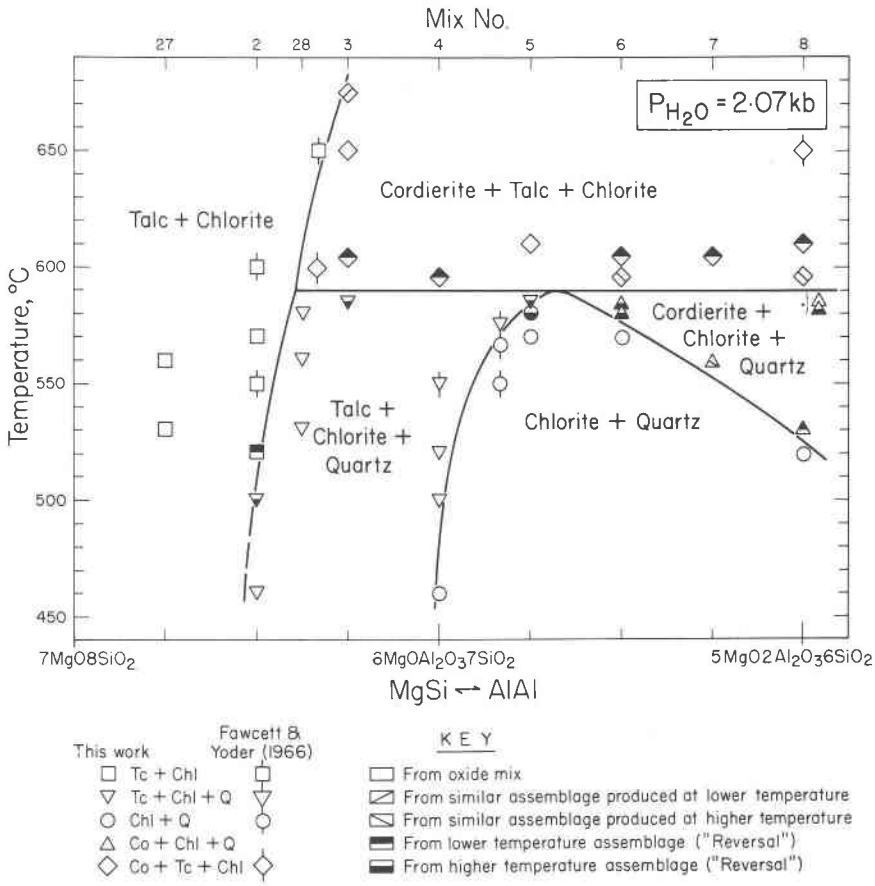

FIG. 3. Critical runs defining the upper stability of chlorite + quartz in Fe-free compositions at P_{H_2O} = 2 kbar. The results are shown on a temperature–composition section along the join anthophyllite ($7MgO \cdot 8SiO_2 \cdot 2H_2O$)–magnesian gedrite ($5MgO \cdot 2Al_2O_3 \cdot 6SiO_2 \cdot 2H_2O$). The symbols represent the assemblages interpreted as stable; additional phases persisted in some runs near boundary curves (see Table 2 for details). All assemblages contained vapor as an additional stable phase.

the range of chlorite compositions extends to that of amesite ($4MgO \cdot 2Al_2O_3 \cdot 2SiO_2 \cdot 4H_2O$), the range of compositions investigated in this work gives no information on the real limit, and in fact, there is some doubt whether the 14 Å chlorite solid solution extends (broken or unbroken) to the amesite composition (Velde, 1973). At the low-alumina end of the chlorite solid-solution range, the configuration of the Tc + Chl + Q and Tc + Chl fields (Fig. 4) requires that the solid solution extend to compositions rather less aluminous than clinochlore ($5MgO \cdot Al_2O_3 \cdot 3SiO_2 \cdot 4H_2O$), and possibly closer to pennine ($5.5MgO \cdot 0.5Al_2O_3 \cdot 3.5SiO_2 \cdot 4H_2O$). However, the compositional range studied is too limited to allow more accurate estimations of the minimum alumina content of 14 Å chlorites. An attempt was made to use Nelson and Roy's data on *d*-spacings for synthetic chlorites to further explore the change in chlorite composition with temperature and bulk chemistry. Although general trends similar to those mentioned above were obtained, the alumina contents were unreasonably high, even allowing for large errors arising from the fact that spacings were determined from routine diffractograms. Application of Albee's (1962, Fig. 5, p. 867) equation for natural chlorites resulted in unreasonably low alumina contents, as expected from earlier experiences (Gillery, 1959; Albee, 1962).

The configuration of talc-bearing fields with respect to bulk composition (Figs. 3 and 4) requires that talc has a significant alumina content, as previously noted by Fawcett and Yoder (1966, p. 374). In fact, it can be deduced graphically from Figures 3 and 4 that the talc contains up to 2.2 atom percent

Al/(Al+Mg+Fe), or 4.2 weight percent Al_2O_3. This is confirmed by the alumina contents determined from the measurements of talc *c* dimensions, using the 2 kbar curve of Fawcett and Yoder (1966, Fig. 5, p. 375). A maximum content of 4.0 weight percent Al_2O_3 was determined (runs 19 and 67 at 585°C). The present work and the evidence from analyses of natural talc strongly support Fawcett and Yoder's suggestion that the maximum alumina content of talc is about 4.0 weight percent.

Compositions with Fe/(Fe+Mg) = 0.5

Critical results for these compositions are listed in Table 3, and are interpreted on a temperature–composition projection along the join FeMg-anthophyllite ($3.5MgO \cdot 3.5FeO \cdot 8SiO_2 \cdot 2H_2O$)—FeMg-gedrite ($2.5MgO \cdot 2.5FeO \cdot 2Al_2O_3 \cdot 6SiO_2 \cdot 2H_2O$) in Figure 5. The symbols represent the assemblages interpreted as stable; additional phases persisted in some runs near boundary curves (Table 3). All assemblages contained water as an additional stable phase.

Below approximately 595°C the sequence of chlorite + quartz assemblages with increasing bulk alumina content is Tc + Mt + Chl + Q, Mt + Chl + Q, Chl + Q, Co + Chl + Q—rather similar to the situation for Fe-free compositions except for the modifications introduced by the occurrence of magnetite. For runs of long duration at or above 600°C, the assemblage Oa + Co + Tc + Mt results. The pair chlorite + quartz thus becomes unstable above about 595°C. This boundary was confirmed by three reversal experiments (runs 154, 183B, 194) including one (154) in which the higher temperature assem-

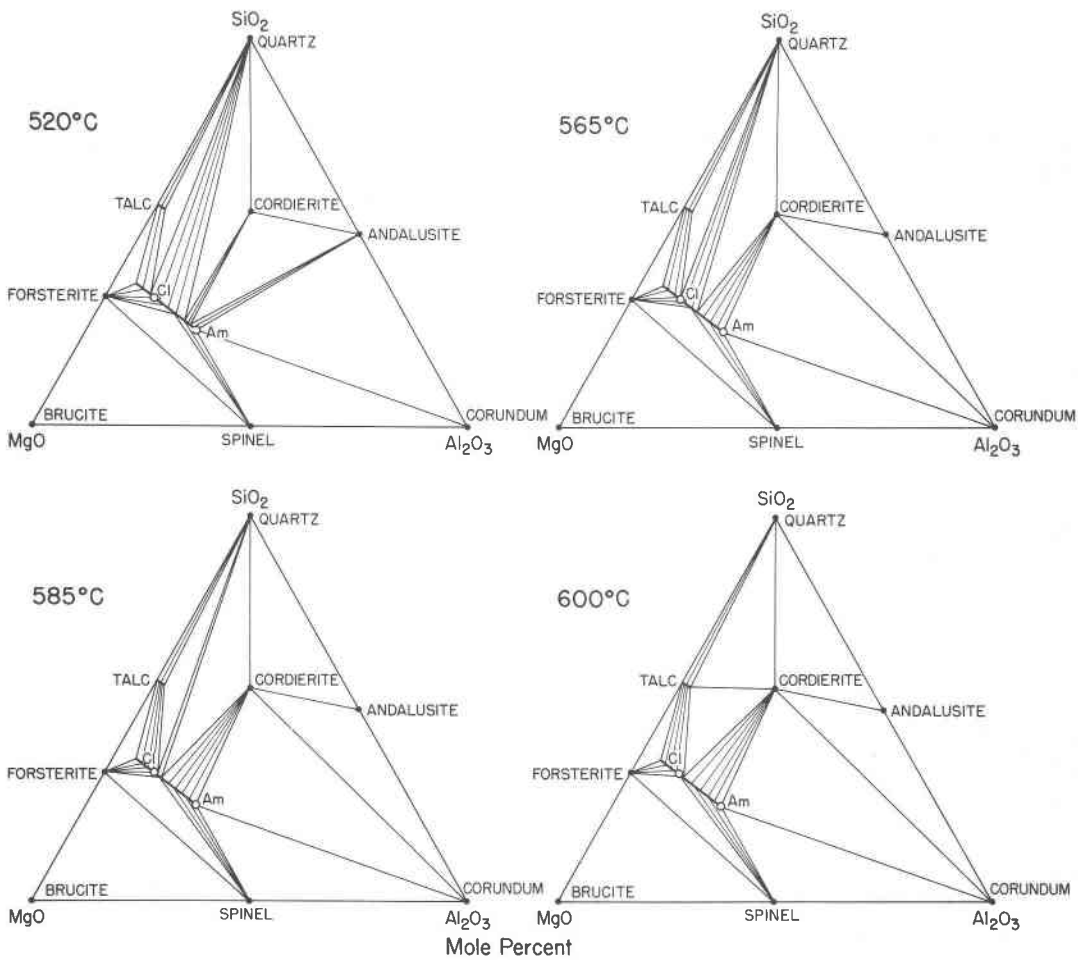

FIG. 4. Isothermal projections in the system $MgO–Al_2O_3–SiO_2–H_2O$ at P_{H_2O} = 2 kbar. The compatibility triangles have been completed by incorporating the data of Yoder (1952), Roy and Roy (1955) and Seifert and Schreyer (1970), and Seifert (1973). Abbreviations: Cl, clinochlore; Am, amesite.

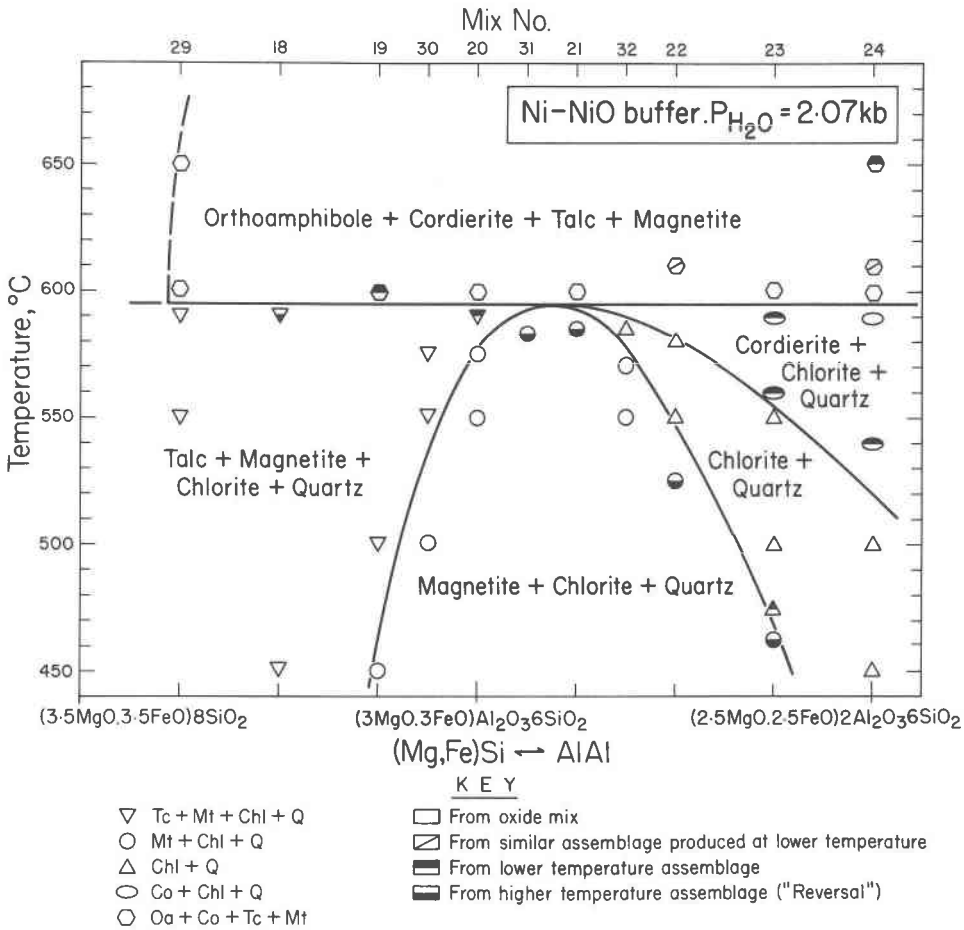

FIG. 5. Critical runs defining the upper stability of chlorite + quartz in compositions with Fe/(Fe + Mg) = 0.5 at P_{H_2O} = 2.07 kbar. The results are shown on a temperature–composition section along the join FeMg-anthophyllite ($3.5MgO \cdot 3.5FeO \cdot 8SiO_2 \cdot 2H_2O$)–FeMg-gedrite ($2.5MgO \cdot 2.5FeO \cdot 2Al_2O_3 \cdot 6SiO_2 \cdot 2H_2O$). The symbols represent the assemblages interpreted as stable; additional phases persisted in some runs near boundary curves (see Table 3 for details). All assemblages contained vapor as an additional stable phase.

blage Oa + Co + TC + Mt was apparently completely replaced by the lower temperature assemblage Tc + Mt + Chl + Q.

The replacement of the chlorite + quartz-bearing assemblages by the higher-temperature assemblage Oa + Co + Mt is probably deceptively simple for the following reason. Ignoring for the moment H_2O as a phase or a component, if the boundary between Oa + Co + Tc + Mt and the lower-temperature assemblages represents isobaric univariant equilibrium, the phase rule requires that only five ($P = C + 1 - 1$) different phases may coexist at the boundary (Fe_2O_3 is the fifth component). Figure 5 shows that six different apparently stable solid phases coexist at the boundary—a situation that can only arise in the present system if the equilibrium is isobarically invariant. That the conditions for this set of experiments happened to coincide with those of the invariant point involving chlorite, quartz, orthorhombic amphibole, cordierite, talc, and magnetite would seem to be unconvincingly fortuitous, and other possibilities are discussed below.

The results of a Schreinemakers' analysis, depicted in Figure 6, show the distribution of all possible univariant curves around the invariant point involving the above six phases plus a vapor (H_2O) phase. The precise composition of phases used in the analysis (see Figure 6 caption) were chosen as reasonable approximations of those expected at the boundary between the Oa + Co + Tc + Mt field and the Tc + Mt + Chl + Q field (see later discussion of mineral compositions). Because of solid-solution ranges, par-

ticularly in chlorite, cordierite, and orthorhombic amphibole, the chemographic relationships between the seven phases will vary with bulk composition, and in some cases, possible variations from the compositions chosen for the above treatment cause the Schreinemakers' solution to differ slightly from that obtained in Figure 6. Such alternative solutions were explored, however, and it was found that the differences do not, in general, affect the discussion below.[4]

Returning to the Schreinemakers' solution of Figure 6, it can be deduced that to first produce orthorhombic amphibole and cordierite from chlorite + quartz assemblages, two univariant curves must be crossed—either (Co) and then (Tc), or (Oa) and then (Chl). The fact that the assemblage chlorite plus quartz is apparently unstable in orthorhombic amphibole-bearing assemblages, and the fact that, although cordierite and orthorhombic amphibole both appear within a few degrees above 595°C, cordierite is generally recognized before orthoamphibole in the progress of a run, would suggest that (Oa) and (Chl) are the reactions responsible for the assemblage Oa + Co + Tc + Mt. The compatibility diagrams for areas between the curves of Figure 6 have been constructed, but are not reproduced here because of perspective problems in small diagrams. For the bulk compositions investigated, the sequence of stable assemblages with increasing temperature should be Tc + Mt + Chl + Q (or Mt + Chl + Q; or Chl + Q; or Co + Chl + Q), Co + Tc + Mt + Q (or Co + Tc + Mt + Chl for the very aluminous compositions), Oa + Co + Tc + Mt. Apparently then, the assemblage Co + Tc + Mt + Q (or Co + Tc + Mt + Chl) is stable over a narrow range, in the order of 10–20°C (Fig. 5), between the upper stability of chlorite + quartz assemblages and the lower stability of the Oa + Tc + Mt assemblage. The width of this temperature interval is evidently so narrow as to prevent the field from being easily resolved experimentally, although the early appearance of cordierite relative to orthorhombic amphibole in the present runs may well have been a real indication of its predicted existence. Further, considering the small temperature interval, one may presume also that either the present experiments have been conducted at pressures close to the invariant

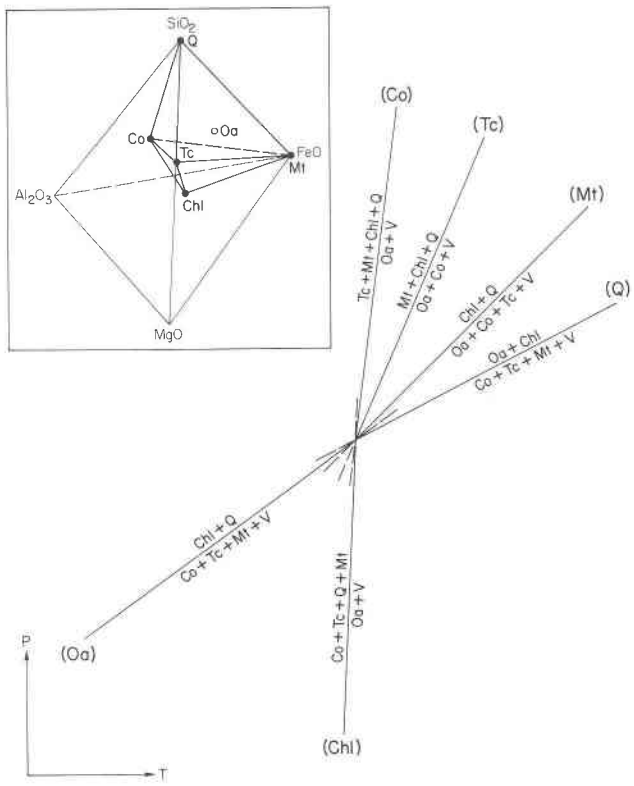

FIG. 6. Schreinemakers' analysis of the invariant point involving chlorite ($3MgO \cdot 2FeO \cdot Al_2O_3\ SiO_2 \cdot 4H_2O$–clinochlore$_{60}$daphnite$_{40}$), anhydrous Mg cordierite ($2MgO \cdot 2Al_2O_3 \cdot 5SiO_2$), talc ($3MgO \cdot 4SiO_2 \cdot 2H_2O$), orthorhombic amphibole ($15FeO \cdot 10MgO \cdot 3Al_2O_3 \cdot 29SiO_2 \cdot 4H_2O$ = FeMg anthophyllite$_{80}$FeMg gedrite$_{20}$), quartz (SiO_2), magnetite (Fe_3O_4), and vapor (H_2O). For each curve the label in parentheses indicates the absent phase for the particular reaction. The vapor-absent curve is omitted as it cannot be shown on the accompanying diagram. Abbreviations as for Tables 2 and 3.

point shown in Figure 6, or the univariant curves (Oa) and (Chl) are closely adjacent, and by implication, (Co), (Tc), and (Mt) are also closely adjacent.

Figure 5, therefore, is probably incomplete, and the nature and configuration of assemblage fields replacing chlorite + quartz fields with increasing temperature are probably more like those shown schematically in Figure 7. Fields 1 and, in part, 2 are those deduced above, whilst a consideration of the isothermal sections shown in Figure 8 and discussed below seems to require fields 2, 3, 4, and 5.

The phase relationships experimentally determined or inferred above are illustrated by the series of isothermal projections in Figure 8. As discussed for Figure 2, the contents of the $FeO–MgO–Al_2O_3–SiO_2$ tetrahedron are projected onto the $MgO–Al_2O_3–SiO_2$ face to avoid many of the problems of apparent crossing of tie lines that would result from other more

[4] For example, when using an orthorhombic amphibole composition that is significantly more Fe- or Al-rich than used in the treatment of Figure 6, the solution is similar except that the sequence of curves (Tc) and (Co) are interchanged, and the reactions across them are modified to Co + Mt + Chl + Q = Oa + H_2O, and Mt + Chl + Q = Oa + Tc + H_2O respectively.

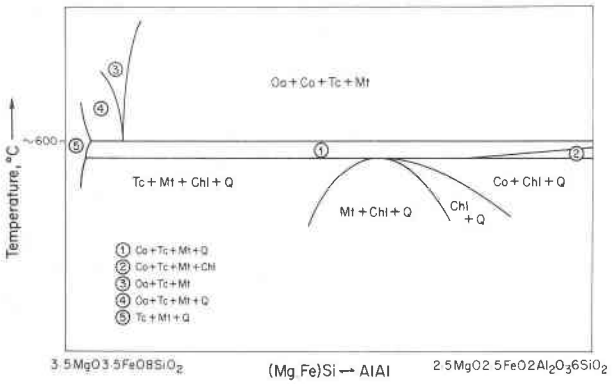

FIG. 7. Schematic configuration of stability fields near the upper thermal stability of chlorite + quartz. Fields (1) to (5) were not experimentally delineated, but are required from other considerations—see text.

familiar projections [*e.g., AFM, A(F,M)S*]. It should be remembered that for assemblages containing magnetite, tie lines connect other members of the assemblage to magnetite, assumed for the purposes of this discussion to lie at the FeO apex.[5] Thus, in terms of MgO–FeO–Al_2O_3–SiO_2, the apparent three-phase fields are four-phase volumes, and two-phase fields are really three-phase triangles. Unlike the projections for the Fe-free compositions discussed earlier, no attempt has been made in Figure 8 to show all possible assemblages for Fe-bearing compositions. This is partly because much of the necessary detailed information is not available, although some data are in hand (*e.g.* Akella and Winkler, 1966; Hsu, 1968; Hsu and Burnham, 1969). To depict satisfactorily the complete phase relationships ev' n for P_{H_2O} = 2 kbar and NNO requires a three-dimensional model of the MgO–FeO–Al_2O_3–SiO_2 tetrahedron or a much more lengthy series of projections.

In four-component systems it is difficult to deduce the compositions of coexisting phases from tie-line orientations. It is also unfortunate that most products were too fine-grained to analyze with the electron microprobe. Nevertheless, some useful observations on the chemistry of coexisting phases can still be made and are elaborated below.

As in the assemblages from Fe-free mixes, the range of compositions of chlorite in equilibrium with quartz (only) contracts with increasing temperature. As shown by the solid bar in Figure 8, the compositions can be defined, because the chlorites must have the same Fe/(Fe + Mg) = 0.5 as the mixes. Furthermore, it can be seen that the range decreases with increasing temperature whilst embracing progressively less aluminous chlorite compositions, until at 595°C, the upper stability of chlorite + quartz, the chlorite is close to $daphnite_{50}clinochlore_{50}$. It is of some interest to note that the chlorite at the upper thermal stability of the pair chlorite + quartz in Fe-free compositions (Fig. 4) also has a relatively low alumina content ($clinochlore_{86}amesite_{14}$). It can also be deduced that chlorites in equilibrium with quartz + cordierite have Fe/(Fe + Mg) = 0.5, and decrease in alumina content with increasing temperature until, at 595°C, they also reach the composition $daphnite_{50}clinochlore_{50}$. On the other hand, those in equilibrium with magnetite + quartz ± talc have unknown Fe/(Fe + Mg) ratios (but < 0.5), and increase in alumina and Fe/(Fe + Mg) as they approach the $daphnite_{50}clinochlore_{50}$ composition at 595°C. Measurement of basal spacings to estimate alumina contents in chlorites using the data of Nelson and Roy (1958) proved to be unsatisfactory, as were similar attempts for the chlorites from Fe-free runs. It is well known that Fe/Mg ratios in chlorite influence the *b* cell-dimension (*e.g.*, see Bailey, 1972), but there was a very poor resolution of chlorite peaks corresponding to (0*k*0) reflections in the diffractograms of the present products, and estimates of chlorite Fe/(Fe + Mg) ratios from cell dimensions were not practical.

The departure of talc from its ideal Fe- and Al-free composition could not be accurately gauged from the isothermal sections, except that, given the determined extent of the Tc + Mt + Chl + Q and Oa + Co + Tc + Mt assemblages to low alumina compositions (Fig. 5), and allowing for the accommodation (above 600°C) of the even lower alumina assemblage Oa + Tc + Mt + Q (Fig. 7), it would seem that talc Al/(Al + Mg + Fe + Si) probably does not exceed about 1.5 atom percent (2.9 weight percent Al_2O_3), as indicated on Figure 8. The iron content of the talc is also probably low, if the results of Forbes's (1971) experiments on Al-free mixes are applicable. Those results imply that, for P_{H_2O} = 2 kbar, Ni–NiO and temperatures greater than about 500°C, talc is likely to have less than about 5 atom percent Fe/(Fe + Mg). Limited information may be obtained from the diffractograms of the talc-bearing products. As mentioned earlier, Figure 5 of Fawcett and Yoder (1966) shows a regular decrease in talc basal spacing with increasing alumina content. Work on synthetic talc in alu-

[5] As noted in the earlier section on experimental methods, magnetite in stable assemblages above 595°C is apparently pure Fe_3O_4. The other magnetites may contain up to 10 percent hercynite component, but this does not seriously affect the ensuing discussion.

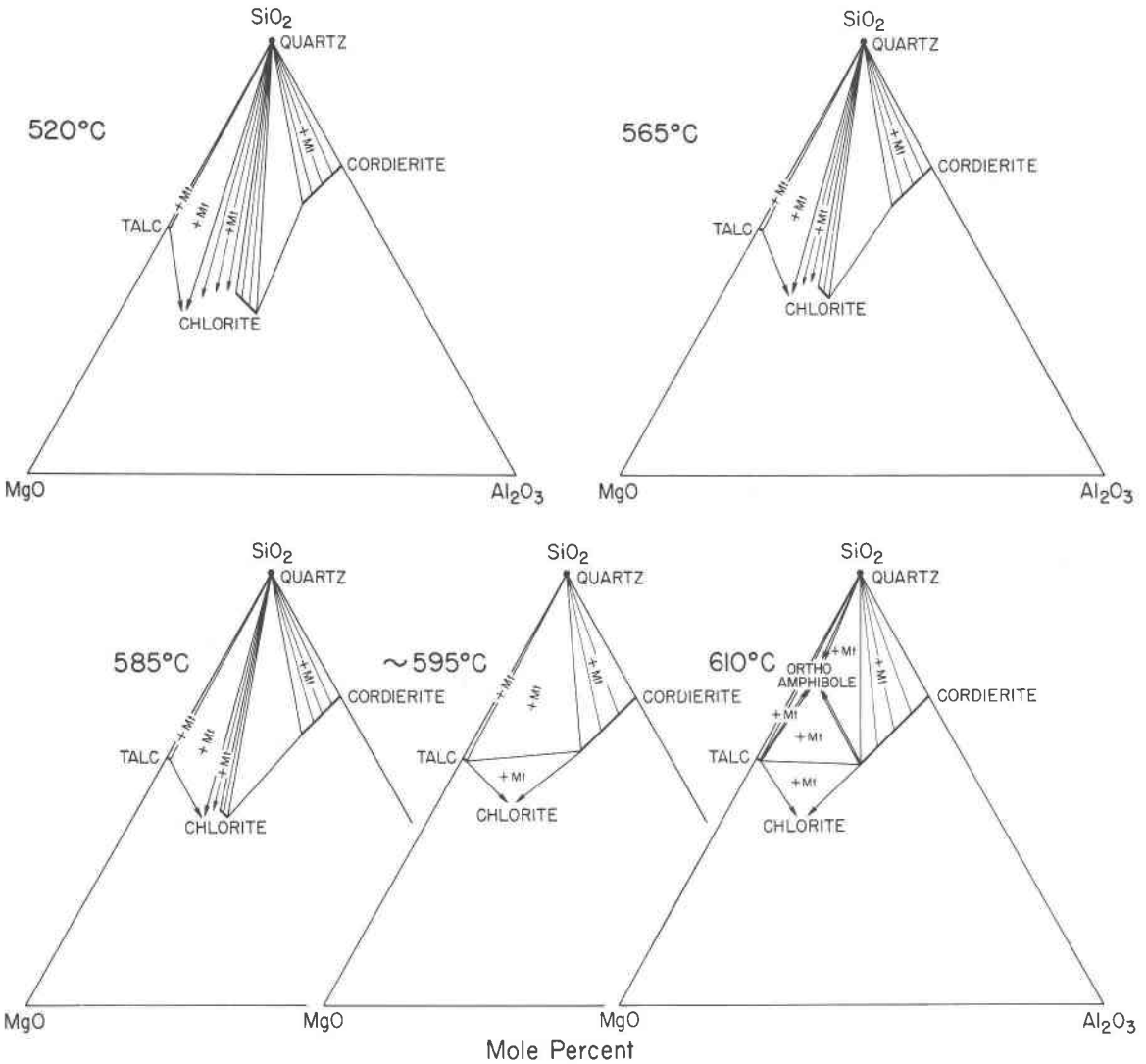

FIG. 8. Isothermal projections from $FeO-H_2O$ in the Ni/NiO-buffered system $MgO-FeO-Al_2O_3-SiO_2-H_2O$ at P_{H_2O} = 2 kbar, for bulk compositions with Fe/(Fe + Mg) = 0.5. With the exception that some data of McOnie *et al.* (1975) have been incorporated on the low MgO side of the diagrams, the projections illustrate only the phase relations interpreted from Figs. 5 and 7, and are therefore grossly incomplete. Chlorites in equilibrium with quartz (heavy line) have Fe/(Fe + Mg) = 0.5. The assemblages near the left and right sides of the diagrams also contain magnetite as indicated.

mina-free charges (Forbes, 1969) suggests that increasing Fe/(Fe + Mg) in talc has the opposite effect and increases the talc *c*-dimension. Hence, these two pieces of information allow estimates of minimum values for weight percent Al_2O_3 and Fe/(Fe + Mg) in talc produced in the present experiments. Given this limitation, the highest atom percent Fe/(Fe + Mg) in talc (produced at 450°C) was 4.3, and Fe/(Fe + Mg) decreased with increasing temperature as predicted by Forbes (1971), until above 600°C no iron was detected. The talc produced below 600°C contained < 1.4 weight percent Al_2O_3; above 600°C it contained < 2.7 weight percent Al_2O_3.

Cordierite in equilibrium with chlorite + quartz will have the same Fe/(Fe + Mg) = 0.5 value as the starting mix. The work of McOnie *et al.* (1975) on the upper stability of chlorites of the clinochlore–daphnite solid-solution series at P_{H_2O} = 2 kbar (Ni–NiO) implies that at 600°C the field for the assemblage Co + Mt + Q extends to within a few atom percent Fe/(Fe + Mg) of pure Mg–cordierite. It is therefore considered that cordierite in the assemblage Oa + Co + Tc + Mt,

and also in the assemblage Oa + Co + Q + Mt (inferred for compositions with slightly less MgO) is virtually pure Mg–cordierite, as indicated on Figure 8.

The composition of orthorhombic amphibole in the assemblage Oa + Co + Tc + Mt is much more equivocal. Even if reliable methods were available to relate the composition of intermediate members of the orthorhombic amphibole solid-solution to their unit cell or optical parameters, the necessary data were not readily obtainable from the run products, due to poor resolution of X-ray reflections from the very fine grain-size of individual amphibole crystals. However, a few compositional limits can be inferred. Assuming that the first orthorhombic amphibole to become stable is not alumina-free [and hence the rationale for fields (3), (4), and (5) in Figure 7], a small field for Oa + Tc + Mt + Q should be stable for compositions with very low alumina. Accepting too that the present work has established the extent of the Oa + Co + Mt + Tc assemblage to quite low alumina compositions, the amphibole composition in equilibrium with those two assemblages must have Fe/(Fe + Mg) > 0.5 and must lie on the Tc–Oa line (Fig. 8) or its further extension to higher Fe/(Fe + Mg) and slightly higher Al_2O_3 values. The amphibole therefore, has a composition with Fe/(Fe + Mg) > 0.5, in which the (Fe) anthophyllite component dominates over the (Fe) gedrite component by a ratio of at least 4 to 1.

Assuming that the magnetite contains little or no magnesioferrite component, their approximate hercynite contents, determined using the X-ray determinative method of Turnock and Eugster (1962), were ≤ 10 percent. Magnetite coexisting with talc + chlorite + quartz contained an average of 6 percent hercynite, whilst in the more aluminous magnetite + chlorite + quartz assemblage it contains about 10 percent hercynite; in equilibrium with orthorhombic amphibole + talc, the magnetite is apparently pure Fe_3O_4.

Compositions with Fe/(Fe + Mg) = 0.082 or 0.75

Because relatively few runs were performed on the set of mixes with Fe/(Fe + Mg) = 0.082 and the mix with Fe/(Fe + Mg/ = 0.75, and because many of the run times were not long enough to produce equilibrium assemblages, a comprehensive delineation of stable assemblages in relation to temperature and composition is not possible at this time. However, the results listed in Table 3 indicate that the breakdown temperature for chlorite + quartz in both sets of compositions was again in the vicinity of 590°C. In mixes with Fe/(Fe + Mg) = 0.082, the stable assemblage above this temperature appears to be Co + Tc + Chl (as for the Fe-free compositions), while for compositions having Fe/(Fe + Mg) = 0.75, the stable assemblage at least above 610°C probably contains orthorhombic amphibole, cordierite, and magnetite, with either chlorite or quartz; the latter would be expected if the amphibole-bearing fields of Figure 8 show, approximately, the correct topology.

Discussion

Considering the results of experiments on all mixes, it now seems that at P_{H_2O} = 2 kbar, and at oxygen fugacites defined by the Ni–NiO buffer, the upper stability temperature of chlorite + quartz is virtually independent not only of alumina content, but also of Fe/(Fe + Mg) ratio, and that in the system $MgO–FeO–Al_2O_3–SiO_2–H_2O$ a wide variety of stable assemblages containing chlorite + quartz at lower temperatures will become unstable at 590 ± 10°C, yielding cordierite-bearing assemblages. Therefore, a series of temperature–composition projections embracing the field of chlorite + quartz assemblages along lines of increasing Fe/(Fe + Mg) ratio will have forms similar to those already depicted (Figs. 3 and 5) along lines of increasing alumina content at constant Fe/(Fe + Mg). This is a *TX* projection on to the line $6MgO \cdot Al_2O_3 \cdot 7SiO_2–6FeO \cdot Al_2O_3 \cdot 7SiO_2$ joining orthorhombic amphiboles of intermediate alumina content (Fig. 9). Only the results critical to the upper stability of chlorite + quartz are plotted. The point at Fe/(Fe + Mg) = 1.0 is deduced from Turnock (1960, Figure 40, p. 103), and represents the temperature where the chlorite–quartz tie-line would become unstable in Ni/NiO-buffered assemblages in the system $FeO–Al_2O_3–SiO_2–H_2O$ at 2 kbar total pressure. The assemblages stable above and below the chlorite + quartz breakdown are interpreted from the results of the present experiments, and also, at the high Fe/(Fe + Mg) end, from those of Turnock (1960). The composition of mix 13 does not lie precisely in the projection plane, but is sufficiently close to be useful in determining the field boundary shown. The boundary curves are shown schematically, because in most cases the experimental data are as yet still too sparse for more accurate estimates. Where the slope of a boundary could not be reasonably estimated, it is shown as vertical.

The chlorite + quartz upper stability temperature of 590 ± 10°C is obviously only valid for the bulk chemistry and physical conditions of the experiments. For example, addition of K_2O to the system $MgO–FeO–Al_2O_3–SiO_2–H_2O$ will lower this temper-

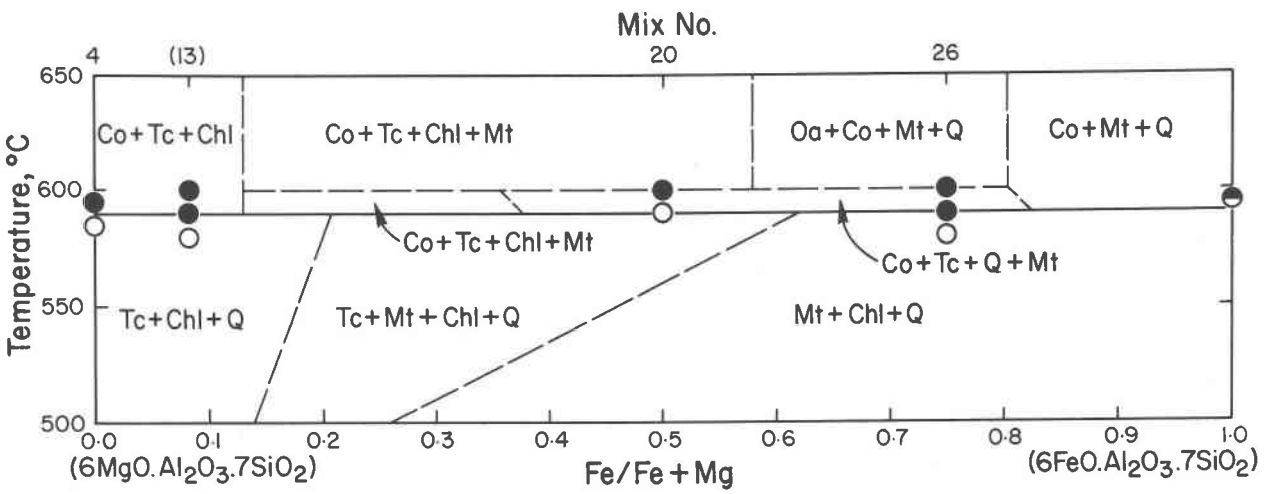

FIG. 9. Largely schematic temperature–composition section at P_{H_2O} = 2 kbar along a line $6MgO \cdot Al_2O_3 \cdot 7SiO_2$–$6FeO \cdot Al_2O_3 \cdot 7SiO_2$ joining orthorhombic amphiboles of intermediate alumina content. Results of runs delineating the stability of chlorite + quartz are indicated. Circles, chlorite + quartz assemblages interpreted as stable; dots, chlorite + quartz unstable, and assemblage contains cordierite ± orthorhombic amphibole; the plot at Fe/(Fe + Mg) = 1 is deduced from Turnock (1960, Fig. 40, p. 103). Other boundaries were inserted after consideration of results of all runs, but are diagrammatic only, the number of runs performed and the range of mix compositions being inadequate for more precise delineation. Vertical boundaries are inserted where the sign of the slope could not be reasonably guessed.

ature; the work of Seifert (1970) and Bird and Fawcett (1973) on part of the system K_2O–MgO–Al_2O_3–SiO_2–H_2O indicates that at 2 kbar total pressure chlorite + quartz will react with muscovite at some 80°C below this temperature to produce cordierite + phlogopite + vapor. Another example is found in the recent work of Liou *et al.* (1974), whose experiments on natural rock powders show that the presence of CaO can lower the chlorite + quartz upper stability temperature by at least 40°C from that determined in the present experiments. At higher pressures the chlorite + quartz breakdown temperature will increase by the order of about 25°C/kbar for Fe-free compositions (Fawcett and Yoder, 1966). An increase in oxygen fugacity above that corresponding to the Ni–NiO buffer would be expected to significantly decrease the chlorite + quartz breakdown temperature, and lower f_{O_2} values might produce less significant changes in chlorite + quartz upper stability (Turnock, 1960, Fig. 40, p. 103).[6] Important changes in stability of other phases could also be expected at oxygen fugacities different from those of this experiment; for example, at fugacities equivalent to the quartz–fayalite–magnetite buffer, some of the cordierite fields delineated in the present work could be infringed upon by garnet–cordierite fields (Hsu, 1968; and Hsu and Burnham, 1969).

Application to natural assemblages

As discussed above, the physiochemical parameters governing the upper thermal stability of natural chlorite + quartz assemblages only approximate those responsible for the assemblages produced experimentally, and hence the results of the present studies should only be applied to natural assemblages with caution.

Some of the rocks whose compositions most closely resemble the relatively simple MgO–FeO–Al_2O_3–SiO_2–H_2O composition of the experimental system are the so-called "cordierite–anthophyllite rocks" described from a wide variety of localities. The occurrence of the cordierite–anthophyllite assemblages has been commonly ascribed to isochemical "contact" metamorphism (Vallance, 1967; Spence, 1969) or regional metamorphism (Froese, 1969) of chlorite-rich rocks. The peculiar chemical composition of the chlorite-rich rocks is often attributed to hydrothermal alteration of volcanics, sometimes associated with base-metal sulfide mineralization (Spence, 1969; Froese, 1969); other authors have suggested that some localities have

[6] More significant changes in the breakdown temperature with increasing f_{O_2} are indicated by Akella and Winkler's (1966) experiments in the *QFM* field. However, these experiments were conducted on amphibole-seeded charges of natural chlorite + quartz, and comparison with the work in the synthetic FeO–MgO–Al_2O_3–SiO_2 system should be made with some caution.

derived their unusually MgO- and FeO-rich compositions by metasomatism (Eskola, 1914) or by segregation and removal of the granitic products of differential melting (Eskola, 1933, Grant, 1968, Lal and Moorhouse, 1969). Whatever the origin of the unusual chemical compositions, it is generally accepted that metamorphism is responsible for the cordierite–anthophyllite assemblages, and many of them are very similar to those produced in the present experiments. For example, the chlorite + quartz assemblages of the hydrothermal-alteration pipes in silicic volcanics of the Noranda-Rouyn Cu-Zn sulfide deposits in Quebec are replaced close to the Lac Dufault granodiorite by assemblages of the type orthorhombic amphibole + cordierite + magnetite + chlorite ± biotite ± quartz (Spence, 1969). The progression is quite similar to the experimental observations, except for the presence of K_2O indicated by the occurrence of biotite. Thus, the results of the present studies could, with suitable reservations, be used to significantly contribute to the evaluation of metamorphic conditions in this and in many other areas containing cordierite–anthophyllite assemblages.

The introductory remarks noted that the results of the present work may also be useful in establishing certain limits for metamorphic conditions experienced by rocks whose compositions are more divergent from those discussed above. For example, in view of the possible persistence to relatively high temperatures (approaching 600°C, as established in these experiments) of chlorite + quartz assemblages with suitable bulk composition, it is of interest to note that, in some of the high-grade pelitic assemblages of the (admittedly higher pressure) Whetstone Lake area (Carmichael, 1970), mutually stable chlorite and quartz are observed to persist almost to the sillimanite isograd (kyanite ⇄ sillimanite), and have evidently been replaced by orthorhombic amphibole–cordierite assemblages just below the somewhat higher-grade sillimanite–garnet–biotite isograd (Carmichael, 1970, p. 157 and 181). One may speculate more generally that chlorite in quartz-bearing assemblages of many high-grade metamorphic rocks may not necessarily all be retrograde and that, as has sometimes been suggested from petrographic evidence, (*e.g.* Green, 1963), chlorite + quartz assemblages may be stable in some rocks to at least the middle of the amphibolite or hornblende hornfels facies, or higher.

Acknowledgments

This work was supported by research grants from the National Research Council of Canada to the second author and also to J. Gittins. We thank Mr. I. Davies for assistance with equipment maintenance and G. M. Anderson, R. S. James, B. Velde, and J. Chernosky, Jr., for comments on earlier versions of this paper.

References

Akella, J. and H. G. F. Winkler (1966) Orthorhombic amphiboles in some metamorphic reactions. *Contrib. Mineral. Petrol.* **12,** 1–12.

Albee, A. L. (1962) Relationships between the mineral association, chemical composition and physical properties of the chlorite series. *Am. Mineral.* **47,** 851–870.

Bailey, S. W. (1972) Determination of chlorite compositions by X-ray spacings and intensities. *Clays Clay Minerals,* **20,** 381–388.

Bird, G. W. and J. J. Fawcett (1973) Stability relations of Mg–chlorite–muscovite and quartz between 5 and 10 Kb water pressure. *J. Petrol.* **14,** 415–428.

Carmichael, D. M. (1970) Intersecting isograds in the Whetstone Lake Area, Ontario. *J. Petrol.* **11,** 141–181.

Chernosky, J. V., Jr. (1975) The stability of the assemblage clinochlore + quartz at low pressure (abstr.). *Trans. Am. Geophys. Union,* **56,** 466.

Coombs, D. S. (1954) The nature and alteration of some Triassic sediments from Southland, New Zealand. *Trans. R. Soc. New Zealand,* **82,** 65–109.

Eisenhart, C. (1968) Expression of the uncertainties of final results. *Science,* **160,** 1201–1204.

Eskola, P. (1914) On the petrology of the Orijärvi region in southwestern Finland. *Comm. Geol. Finlande Bull.* **40,** 1–277.

——— (1933) On the differential anatexis of rocks. *Comm. Geol. Finlande Bull.* **103,** 12–25.

Eugster, H. P. and D. R. Wones (1962) Stability relations of the ferruginous biotite, annite. *J. Petrol.* **3,** 82–125.

Fawcett, J. J. and H. S. Yoder, Jr. (1966) Phase relationships of chlorites in the system $MgO–Al_2O_3–SiO_2–H_2O$. *Am. Mineral.* **51,** 353–380.

Fleming, P. D. and J. J. Fawcett (1974) Upper stability of chlorite + quartz assemblages in the Ni/NiO-buffered system $MgO–FeO–Al_2O_3–SiO_2–H_2O$ at 2 Kb water pressure (abstr.). *Trans. Am. Geophys. Union,* **55,** 479.

Forbes, W. C. (1969) Unit-cell parameters and optical properties of talc on the join $Mg_3Si_4O_{10}(OH)_2–Fe_3Si_4O_{10}(OH)_2$. *Am. Mineral.* **54,** 1399–1408.

——— (1971) Iron content of talc in the system $Mg_3Si_4O_{10}(OH)_2–Fe_3Si_4O_{10}(OH)_2$. *J. Geol.* **71,** 63–74.

Froese, E. (1969) Metamorphic rocks from the Coronation Mine and surrounding area. In, A. R. Byers, Ed., *Symposium on the Geology of Coronation Mine, Saskatchewan, Geol. Surv. Can. Pap.* **68-5,** 55–57.

Gillery, F. H. (1959) X-ray study of synthetic Mg–Al serpentines and chlorites. *Am. Mineral.* **44,** 143–152.

Grant, J. A. (1968) Partial melting of common rocks as possible sources of cordierite–anthophyllite-bearing assemblages. *Am. J. Sci.* **266,** 908–931.

Green, J. C. (1963) High-level metamorphism of pelitic rocks in northern New Hampshire. *Am. Mineral.* **48,** 991–1023.

Grieve, R. A. F. and J. J. Fawcett (1974) The stability of chloritoid below 10 kb P_{H_2O}. *J. Petrol.* **15,** 113–139.

Hsu, L. C. (1968) Selected phase relationships in the system Al–Mn–Fe–Si–O–H: A model for garnet equilibria. *J. Petrol.* **9,** 40–83.

——— and C. W. Burnham (1969) Phase relationships in the

system $Fe_3Al_2Si_3O_{12}$–$Mg_3Al_2Si_3O_{12}$–H_2O at 2.0 kilobars. *Geol. Soc. Am. Bull.* **80,** 2393–2408.

JAMES, R. S., A. C. TURNOCK AND J. J. FAWCETT (1976) Stability and phase relations of iron chlorite below 8.5 kb P_{H_2O}. *Contrib. Mineral. Petrol.* **56,** 1–25.

LAL, R. K. AND W. W. MOORHOUSE (1969) Cordierite–gedrite rocks and associated gneisses of Fishtail Lake, Harcourt Township, Ontario.*Can. J. Earth Sci.* **6,** 145–165.

LIOU, J. G., S. KUNIYOSHI AND K. ITO (1974) Experimental studies of the phase relations between greenschist and amphibolite in a basaltic system. *Am. J. Sci.* **274,** 613–632.

MCONIE, A. W., J. J. FAWCETT AND R. S. JAMES (1975) The stability of intermediate chlorites of clinochlore–daphnite series at 2 kbar P_{H_2O}. *Am. Mineral.* **60,** 1047–1062.

NELSON, B. W. AND R. ROY (1954) New data on the composition and identification of the chlorites. *Proc. 2nd Natl. Conf., Clays Clay Miner. Natl. Res. Council Publ.* **327,** 335–348.

——— AND ——— (1958) Synthesis of chlorites and their structural and chemical constitution. *Am. Mineral.* **43,** 707–725.

ROY D. M. AND R. ROY (1955) Synthesis and stability of minerals in the system MgO–Al_2O_3–SiO_2–H_2O. *Am. Mineral.* **40,** 147–178.

SEIFERT, F. (1970) Low-temperature compatibility relations of cordierite in haplopelites of the system K_2O–MgO–Al_2O_3–SiO_2–H_2O. *J. Petrol.* **11,** 73–99.

——— (1973) Stability of the assemblage cordierite–corundum in the system MgO–Al_2O_3–SiO_2–H_2O. *Contrib. Mineral. Petrol.* **41,** 171–177.

——— AND W. SCHREYER (1970) Lower temperature stability of Mg cordierite in the range 1–7 kilobars water pressure. A redetermination. *Contrib. Mineral. Petrol.* **27,** 225–238.

SPENCE, A. (1969) Genése des roches à cordiérite–anthophyllite des gisements cupro-zincifères de la region de Rouyn-Noranda, Québec, Canada. *Can. J. Earth Sci.* **6,** 1339–1345.

STIRLAND, D. J., A. G. THOMAS AND N. C. MOORE (1958) Observations on thermal transformations in alumina. *Trans. Brit. Ceram. Soc.* **57,** 69–84.

TURNER, F. J. (1968) *Metamorphic Petrology: Mineralogical and Field Aspects.* McGraw-Hill Inc., New York, 403 p.

TURNOCK, A. C. (1960) The stability of iron chlorites. *Carnegie Inst. Wash. Year Book,* **59,** 98–103.

——— AND H. P. EUGSTER (1962) Fe–Al oxides: Phase relationships below 1000°C. *J. Petrol.* **3,** 533–565.

TUTTLE, O. F. (1949) Two pressure vessels for silicate-water studies. *Geol. Soc. Am. Bull.* **60,** 1727–1729.

VALLANCE, T. G. (1967) Mafic rock alteration and isochemical redevelopment of some cordierite–anthophyllite rocks. *J. Petrol.* **8,** 84–96.

VELDE, B. (1973) Phase equilibria in the system MgO–Al_2O_3–SiO_2–H_2O: chlorites and associated minerals. *Mineral. Mag.* **39,** 297–312.

WINKLER, H. G. F. (1965) *Petrogenesis of Metamorphic Rocks.* Springer-Verlag, Berlin, 220 p.

YODER, H. S., JR. (1952) The MgO–Al_2O_3–SiO_2–H_2O system and the related metamorphic facies. *Am. J. Sci.,* Bowen Vol., 569–627.

Manuscript received, March 24, 1976; accepted for publication, July 22, 1976.